Food Chemistry 385 (2022) 132638

Contents lists available at ScienceDirect

Food Chemistry

journal homepage: www.elsevier.com/locate/foodchem

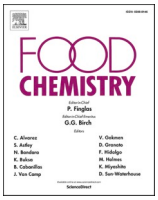

Thermal degradation kinetics and pyrolysis GC–MS study of curcumin

Rashid Masih, Mohammad S. Iqbal *

Department of Chemistry, Forman Christian College, Lahore 54600, Pakistan

ARTICLE INFO

Keywords:
Curcumin
Thermal degradation
Isoconversional analysis
Pyrolysis GC–MS

ABSTRACT

The objective of this work was to study kinetics of thermal degradation of curcumin in ambient–1023 K range and identify degradation products by GC–MS. No weight loss was observed up to ~470 K and two major weight losses occurred beyond this. Sixteen degradation products were identified by GC–MS. Pharmacological properties, including LD_{50}, LC_{50}, gastrointestinal absorption, blood-brain barrier permeation and effect on cytochromes, of the products were calculated using standard software. The LD_{50} values indicated that the degradation products are more toxic than curcumin. All the decomposition products, except 2-methyl-6-(4-methylphenyl)-hept-2-en-4-one, have the potential to cross the blood–brain barrier that can affect brain functions. Twelve of the compounds showed the potential to inhibit the metabolism of xenobiotics and all the compounds appeared to be non-inhibitors of CYP2C9 and CYP3A4 in contrast to curcumin. Thus, this study suggests that the food materials containing curcumin when heated beyond 470 K will produce toxic substances.

1. Introduction

Curcumin, 1,7-bis(4-hydroxy-3-methoxyphenyl) hepta-1,6-diene-3,5-dione, is a yellow-coloured compound abundantly found in turmeric. *Curcuma longa*, turmeric, is a well-known food material. It is one of the common spices used in preparation of several dishes in Pakistan and around the world. It is also used as a herbal supplement for prophylaxis of colon cancer (Volate et al., 2005), food color and cosmetic ingredient (Shang et al., 2019). It has been reported to possess anti-oxidant, anti-inflammatory, anti-cancer and analgesic properties (Chengaiah et al., 2010). Curcumin is an unstable compound (Nelson et al., 2017). Most of the food items containing curcumin are cooked by way of boiling and or frying in oils. This process may alter the status of curcumin, i.e., It may degrade into different substances, which may be hazardous or beneficial for health. There exists little information about the production of degradation products of curcumin and their kinetics at higher temperatures. One of the studies reported formation of deketene curcumin (1,5-bis(4-hydroxy-3-methoxyphenyl)-1,4-pentadiene-3-one) showing a greater anti-cancer activity than curcumin (Dahmke et al., 2014). Vanillin, 4-vinyl guaiacol and ferulic acid have shown to be formed by heating curcumin at 453 K (Esatbeyoglu et al., 2015). In another study kinetics of curcumin degradation has been described as the single step process in two stages with no information on the nature of degradation products (Chen et al., 2014). The present work was planned to thoroughly investigate the effect of heating on curcumin, identify the degradation products by GC–MS in the ambient–1023 K range, determine toxicity profile and study degradation kinetics of its degradation products by an optimized isoconversional method. We hypothesize that curcumin will generate toxic degradation products on heating beyond 470 K.

2. Materials and methods

2.1. Materials

Curcumin (CAS # 458-37-7, SC-20050B, Santa Cruz, USA, purity > 95.0%) and ethanol (CAS # 64–17-5, CAT # 32221, Sigma-Aldrich, Germany, 99.8%), were used as obtained.

2.2. Thermogravimetric analysis (TGA)

Curcumin (~3.63 mg) was placed in alumina cup and analyzed by Simultaneous Thermo Gravimetric Analyzer SDT, Q600 (TA instruments, USA) at 5, 10, 15 and 20 K min^{-1} from ambient to ~1023 K under nitrogen (100 cm^3 min^{-1}). The data were analyzed by Universal Analysis 2000 software, version 5.1.2E (TA Instruments, USA). The weight and temperature calibrations for TGA were carried out according to the instruction manual of the instrument using the reference weights (P/N # 960014.901, TA instruments, USA) and zinc metal (P/N # 960234.901, TA instruments, USA), respectively.

* Corresponding author.
E-mail address: saeediqbal@fccollege.edu.pk (M.S. Iqbal).

https://doi.org/10.1016/j.foodchem.2022.132638
Received 16 November 2021; Received in revised form 2 March 2022; Accepted 3 March 2022
Available online 5 March 2022

Table 1
The decomposition products of curcumin at 303 to 1023 K as identified by GC–MS and their pharmacological properties.

Sr. No.	Compound	Structure	MW (g mol^{-1})	Relative abundance (%) at				LC_{50} [a] Log mol/L	LD_{50} [a] Log mol/kg	Pharmacological properties[b]
				Ambient-583 K	583–633 K	633–773 K	Ambient −1023 K			
1	Phenol (CAS # 108–95-2)		94	6.38	1.81	4.70	2.87	3.5 Exp	2.47 Exp	Gastrointestinal absorption: High BBB permeation: Yes Cytochrome P450 1A2 inhibitor: Yes CYP2C19 inhibitor: No, CYP2C9 inhibitor: No CYP2D6 inhibitor: No, CYP3A4 inhibitor: No
2	1,4-dimethoxy −2-methylbenzene (CAS # 24599–58-4)	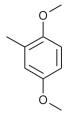	152	3.03	3.36	–	18.17	3.44	1.96	Gastrointestinal absorption: High BBB permeation: Yes Cytochrome P450 1A2 inhibitor: Yes CYP2C19 inhibitor: No, CYP2C9 inhibitor: No CYP2D6 inhibitor: No, CYP3A4 inhibitor: No
3	1-(2-hydroxy-5-methylphenyl) (CAS # 1450–72-2)	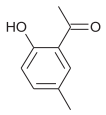	150	5.34	–	–	–	3.85	1.91	Gastrointestinal absorption: High BBB permeation: Yes Cytochrome P450 1A2 inhibitor: Yes CYP2C19 inhibitor: No, CYP2C9 inhibitor: No CYP2D6 inhibitor: No, CYP3A4 inhibitor: No
4	4-ethenyl-2-methoxyphenol	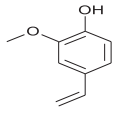	150	21.59	–	–	11.34	4.38	2.13	Gastrointestinal absorption: High BBB permeation: Yes Cytochrome P450 1A2 inhibitor: Yes CYP2C19 inhibitor: No, CYP2C9 inhibitor: No CYP2D6 inhibitor: No, CYP3A4 inhibitor: No
5	2-methoxyphenol (CAS # 90–05-1)	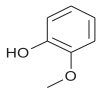	124	24.66	13.46	29.66	18.17	3.27	2.38 Exp	Gastrointestinal absorption: High BBB permeation: Yes Cytochrome P450 1A2 inhibitor: No CYP2C19 inhibitor: No, CYP2C9 inhibitor: No CYP2D6 inhibitor: No, CYP3A4 inhibitor: No
6	4-ethyl-2-methoxyphenol (CAS # 2785–89-9)	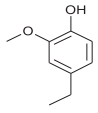	152	4.90	9.90	–	9.97	3.92	2.11	Gastrointestinal absorption: High BBB permeation: Yes Cytochrome P450 1A2 inhibitor: Yes CYP2C19 inhibitor: No, CYP2C9 inhibitor: No CYP2D6 inhibitor: No, CYP3A4 inhibitor: No
7	2-methoxy-6-methylphenol	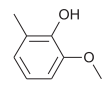	138	-	25.92	9.64	15.55	3.63	2.21	Gastrointestinal absorption: High BBB permeation: Yes Cytochrome P450 1A2 inhibitor: Yes CYP2C19 inhibitor: No, CYP2C9 inhibitor: No

(*continued on next page*)

Table 1 (*continued*)

Sr. No.	Compound	Structure	MW (g mol^{-1})	Relative abundance (%) at				LC_{50} [a] Log mol/L	LD_{50} [a] Log mol/kg	Pharmacological properties[b]
				Ambient-583 K	583–633 K	633–773 K	Ambient −1023 K			
8	4-methoxyphenol (CAS # 150–76-5)	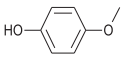	124	–	21.61	21.63	–	3.11 Exp	1.89 Exp	CYP2D6 inhibitor: No, CYP3A4 inhibitor: No Gastrointestinal absorption: High BBB permeation: Yes Cytochrome P450 1A2 inhibitor: No CYP2C19 inhibitor: No, CYP2C9 inhibitor: No CYP2D6 inhibitor: No, CYP3A4 inhibitor: No
9	2-methoxy-4-methylphenol (CAS # 93–51-6)		138	–	13.50	9.78	3.02	3.43	2.27 Exp	Gastrointestinal absorption: High BBB permeation: Yes Cytochrome P450 1A2 inhibitor: No CYP2C19 inhibitor: No, CYP2C9 inhibitor: No CYP2D6 inhibitor: No, CYP3A4 inhibitor: No
10	4-(4-hydroxy-3methoxyphenyl) but-3-en-2-one (CAS # 1080–12-2)	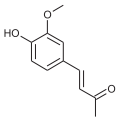	192	–	–	14.65	15.60	4.34	1.66	Gastrointestinal absorption: High BBB permeation: Yes Cytochrome P450 1A2 inhibitor: Yes CYP2C19 inhibitor: No, CYP2C9 inhibitor: No CYP2D6 inhibitor: No, CYP3A4 inhibitor: No
11	4-hydroxy-3-methoxybenzaldehyde (CAS # 121–33-5)	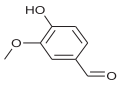	152	–	–	–	0.99	3.12 Exp	1.98 Exp	Gastrointestinal absorption: High BBB permeation: Yes Cytochrome P450 1A2 inhibitor: No CYP2C19 inhibitor: No, CYP2C9 inhibitor: No CYP2D6 inhibitor: No, CYP3A4 inhibitor: No
12	4-(4-hydroxy-3-methoxyphenyl) butan-2-one (CAS # 122–48-5)	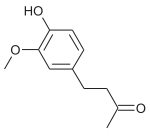	194	–	–	–	5.23	4.18	1.88 Exp	Gastrointestinal absorption: High BBB permeation: Yes Cytochrome P450 1A2 inhibitor: Yes CYP2C19 inhibitor: No, CYP2C9 inhibitor: No CYP2D6 inhibitor: No, CYP3A4 inhibitor: No
13	2-methyl-6-(4-methylphenyl) hept-2-en-4-one (CAS # 38142–58-4)	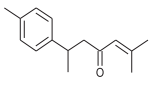	216	–	–	–	1.12	4.99	1.85	Gastrointestinal absorption: High BBB permeation: No Cytochrome P450 1A2 inhibitor: Yes CYP2C19 inhibitor: No, CYP2C9 inhibitor: No CYP2D6 inhibitor: No, CYP3A4 inhibitor: No
14	4-(4-hydroxyphenyl) but-3-en-2-one	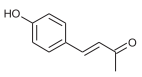	162	–	–	–	1.18	4.44	1.84	Gastrointestinal absorption: High BBB permeation: Yes Cytochrome P450 1A2 inhibitor: Yes CYP2C19 inhibitor: No, CYP2C9 inhibitor:

(*continued on next page*)

Table 1 (*continued*)

Sr. No.	Compound	Structure	MW (g mol^{-1})	Relative abundance (%) at				LC_{50} [a] Log mol/L	LD_{50} [a] Log mol/kg	Pharmacological properties[b]
				Ambient-583 K	583–633 K	633–773 K	Ambient −1023 K			
										No CYP2D6 inhibitor: No, CYP3A4 inhibitor: No
15	2,3-dihydro-1-benzofuran (CAS # 496–16-2)		120	–	–	–	1.48	3.17 Exp	2.09	Gastrointestinal absorption: High BBB permeation: Yes Cytochrome P450 1A2 inhibitor: Yes CYP2C19 inhibitor: No, CYP2C9 inhibitor: No CYP2D6 inhibitor: No, CYP3A4 inhibitor: No
16	3-methylphenol (CAS # 108–39-4)	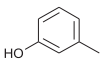	108	–	–	–	1.66	3.29 Exp	2.65 Exp	Gastrointestinal absorption: High BBB permeation: Yes Cytochrome P450 1A2 inhibitor: Yes CYP2C19 inhibitor: No, CYP2C9 inhibitor: No CYP2D6 inhibitor: No, CYP3A4 inhibitor: No
17	(1*E*,6*E*)-1,7-bis(4-hydroxy-3-methoxyphenyl)hepta-1,6-diene-3,5-dione (CAS # 458–37-7)	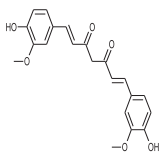	368					6.45	2.56	Gastrointestinal absorption: High BBB permeation: No Cytochrome P450 1A2 inhibitor: No CYP2C19 inhibitor: No, CYP2C9 inhibitor: Yes CYP2D6 inhibitor: No, CYP3A4 inhibitor: Yes

[a]Calculated by use of T.E.S.T software Version 4.2.1 [https://www.epa.gov/chemical-research/toxicity-estimation-software-tool-test].
[b]Calculated by use of SwissADME Methodologies [http://www.swissadme.ch/].

2.3. Degradation kinetics

Thermal degradation kinetics of curcumin was studied by optimized isoconversional (model-independent) method reported by Starink (Eq. 1) (Starink, 2003). The activation energies (*Ea*) values were determined from the slopes of straight-line plots of $\ln(\beta/T^{1.92})$ vs $1000/T$. The degradation mechanism, $g(\alpha)$, was determined by use of the master-plot method, (Eq. (2)) (Turmanova et al., 2008; Iqbal et al., 2016).

$$\ln\left[\frac{\beta}{T^{1.92}}\right] = \text{Const} - 1.0008\frac{E_\alpha}{RT} \tag{1}$$

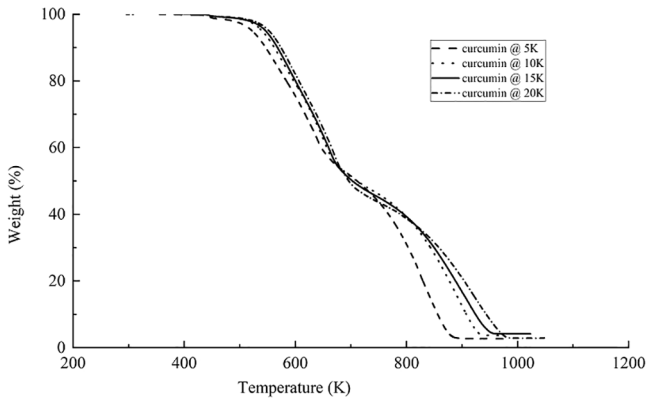

Fig. 1. TGA curves at heating rates 5, 10, 15 and 20 K min^{-1}.

where, R is the general gas constant; β the heating rate; E_a and T are the activation energy and temperature at the degree of conversion (α), respectively.

$$\frac{g(\alpha)}{g(0.5)} = \frac{p(x)}{p(x_{0.5})} \tag{2}$$

where $x = E_a/RT$, $p(x) = \int_x^\infty \frac{e^{-x}}{x^2}\,dx$ and $g(0.5)$ and $p(x_{0.5})$ are theoretical and experimental reaction models at $\alpha = 0.5$, respectively. The theoretical master plots were obtained by plotting $g(\alpha)/g(0.5)$ against α for various $g(\alpha)$ functions (supplementary Table 1) (Janković, 2008). Experimental master plots were obtained by plotting $p(x)/p(x_{0.5})$ against α. The $p(x)$ integral was solved as reported by Starink (Eq. 3) (Starink, 2003; Vyazovkin et al., 2011). Pre-exponential factor (A) was determined by use of compensation effect relationship (Eq. 4) (Vyazovkin et al., 2011).

$$p(x) = e^{(-1.0008x - 0.312)}/x^{1.92} \tag{3}$$

$$\ln A = a + bE_a \tag{4}$$

In Eq. 4 a and b are the compensation parameters, which were determined by model-fitting method using Coats-Redfern equation (Eq. 5) (Coat & Redfern, 1964).

$$\ln\frac{g(\alpha)}{T^2} = \ln\left[\left(\frac{AR}{\beta E_a}\right)\left(1 - \frac{2R\overline{T}}{E_a}\right)\right] - \frac{E_a}{RT} \tag{5}$$

where, $\overline{T}$ is the average experimental temperature. The $g(\alpha)$ models were

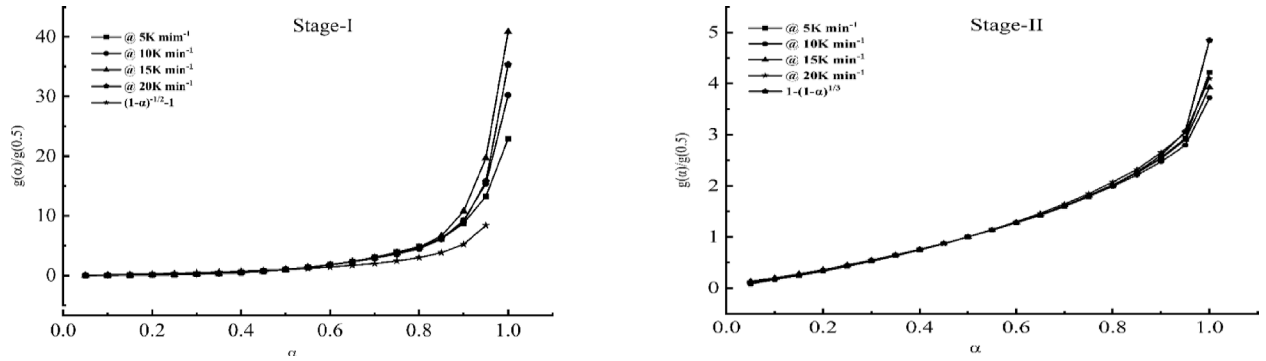

Fig. 2. Determination of Kinetic models for curcumin at stage- I & II: experimental and theoretical master plots.

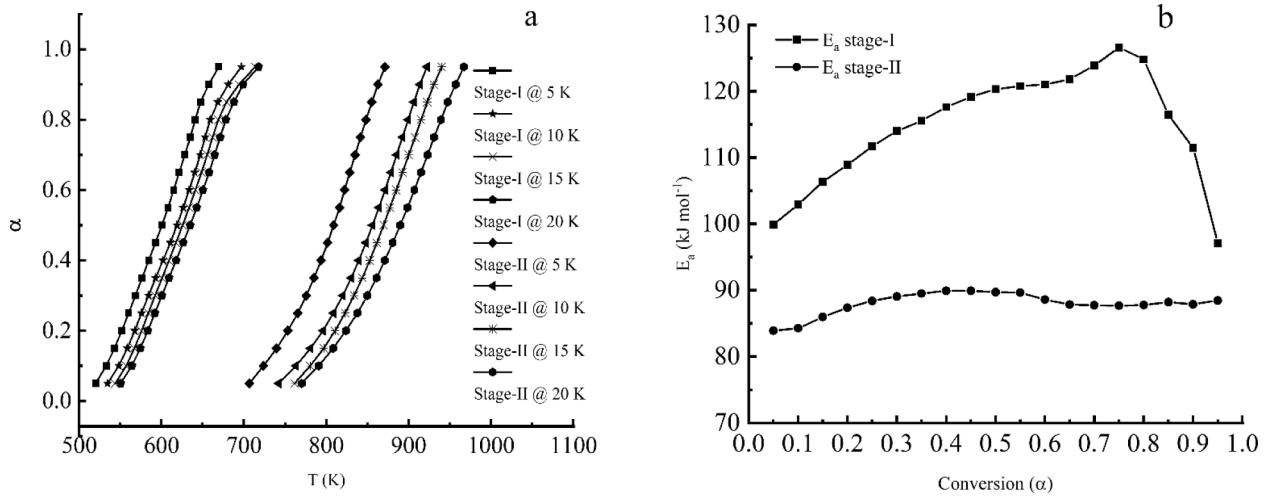

Fig. 3. (a) Temperature vs conversion (T-α) and (b) activation energy vs conversion (E_a - α) plots.

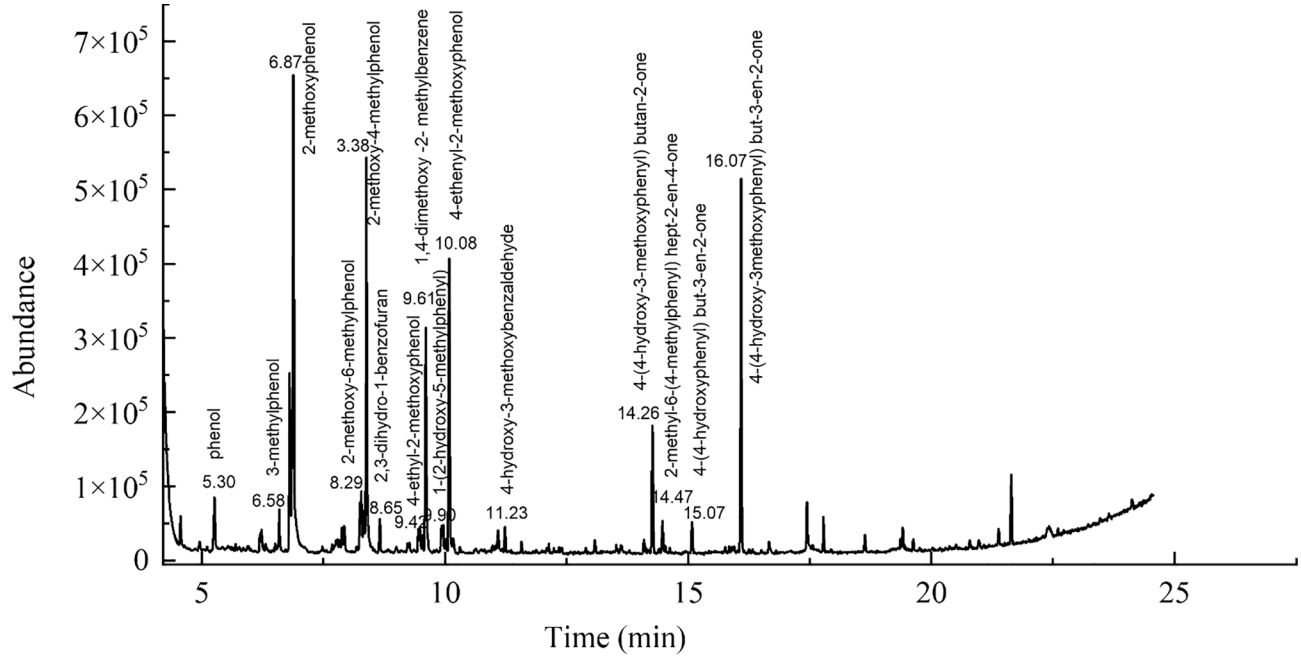

Fig. 4. Chromatogram of pyrolytic products of curcumin collected at ambient to 973 K in ethanol.

Table 2
Mass spectral data of curcumin degradation products.

Retention time (t_R, min)	Molecular ion (amu)	Fragmentation pattern (amu)
5.30	$[C_6H_6O]^+$ m/e = 94	$[C_5H_6]^+$ m/e = 66; $[C_4H_6 + H]^+$ m/e = 55; $[C_3H_6 + H]^+$ m/e = 43; $[C_3H_4]^+$ m/e = 40; $[CO]^+$ m/e = 28;
6.58	$[C_7H_7O]^+$ m/e = 107	$[C_7H_6]^+$ m/e = 90; $[C_6H_4 + H]^+$ m/e = 77; $[C_5H_2 + H]^+$ m/e = 63; $[C_4H_2 + H]^+$ m/e = 51; $[C_3H_2 + H]^+$ m/e = 39
6.87	$[C_7H_8O_2]^+$ m/e = 124	$[C_7H_8O + H]^+$ m/e = 109; $[C_6H_6O + H]^+$ m/e = 95; $[C_6H_8 + H]^+$ m/e = 81; $[C_5H_4 + H]^+$ m/e = 65; $[C_4H_4 + H]^+$ m/e = 53; $[C_3H_2 + H]^+$ m/e = 39; $[CO]^+$ m/e = 28;
8.29	$[C_8H_{10}O_2]^+$ m/e = 138	$[C_8H_{10}O + H]^+$ m/e = 123; $[C_7H_6O + H]^+$ m/e = 107; $[C_6H_6O + H]^+$ m/e = 95; $[C_6H_4 + H]^+$ m/e = 77; $[C_5H_6 + H]^+$ m/e = 67; $[C_4H_6 + H]^+$ m/e = 55; $[C_4H_2 + H]^+$ m/e = 51; $[C_3H_2 + H]^+$ m/e = 39
8.382	$[C_8H_{10}O_2]^+$ m/e = 138	$[C_8H_{10}O + H]^+$ m/e = 123; $[C_6H_6O + H]^+$ m/e = 95; $[C_6H_4 + H]^+$ m/e = 77;$[C_5H_6 + H]^+$ m/e = 67; $[C_4H_6 + H]^+$ m/e = 55; $[C_4H_2 + H]^+$ m/e = 51; $[C_3H_2 + H]^+$ m/e = 39
8.65	$[C_8H_8O]^+$ m/e = 120	$[C_8H_8 + H]^+$ m/e = 105; $[C_7H_6 + H]^+$ m/e = 91; $[C_6H_4 + H]^+$ m/e = 77; $[C_5H_4 + H]^+$ m/e = 65; $[C_4H_2 + H]^+$ m/e = 51; $[C_3H_2 + H]^+$ m/e = 39
9.42	$[C_9H_{12}O_2]^+$ m/e = 152	$[C_9H_{12}O + H]^+$ m/e = 137; $[C_8H_{10}O]^+$ m/e = 122; $[C_6H_6O]^+$ m/e = 94; $[C_6H_6]^+$ m/e = 78; $[C_4H_2 + H]^+$ m/e = 51;
9.61	$[C_9H_{12}O_2]^+$ m/e = 152	$[C_9H_{12}O + H]^+$ m/e = 137; $[C_8H_{10}O]^+$ m/e = 122; $[C_7H_8O + H]^+$ m/e = 109; $[C_7H_6 + H]^+$ m/e = 91; $[C_6H_4 + H]^+$ m/e = 77; $[C_5H_4 + H]^+$ m/e = 65; $[C_4H_2 + H]^+$ m/e = 51
9.90	$[C_9H_{10}O_2]^+$ m/e = 150	$[C_9H_{10}O + H]^+$ m/e = 135; $[C_8H_{10} + H]^+$ m/e = 107; $[C_6H_4 + H]^+$ m/e = 77; $[C_4H_2 + H]^+$ m/e = 51; $[C_3H_2 + H]^+$ m/e = 39
10.08	$[C_9H_{10}O_2]^+$ m/e = 150	$[C_9H_{10}O + H]^+$ m/e = 135; $[C_8H_6O]^+$ m/e = 118; $[C_8H_{10} + H]^+$ m/e = 107; $[C_6H_8 + H]^+$ m/e = 81; $[C_6H_4 + H]^+$ m/e = 77; $[C_5H_2 + H]^+$ m/e = 63; $[C_4H_2 + H]^+$ m/e = 51;
11.23	$[C_8H_8O_3]^+$ m/e = 152	$[C_8H_8O_2 + H]^+$ m/e = 137; $[C_8H_{10}O + H]^+$ m/e = 123; $[C_7H_8O + H]^+$ m/e = 109; $[C_6H_6O + H]^+$ m/e = 95; $[C_6H_8 + H]^+$ m/e = 81; $[C_5H_2 + H]^+$ m/e = 63; $[C_4H_2 + H]^+$ m/e = 51
14.26	$[C_{11}H_{14}O_3]^+$ m/e = 194	$[C_{11}H_{14}O2 + H]^+$ m/e = 179; $[C_{11}H_{12}O + H]^+$ m/e = 161; $[C_{10}H_{14}O + H]^+$ m/e = 151; $[C_9H_{12}O + H]^+$ m/e = 137; $[C_8H_6O + H]^+$ m/e = 119; $[C_8H_{10} + H]^+$ m/e = 107; $[C_7H_6 + H]^+$ m/e = 91; $[C_6H_4 + H]^+$ m/e = 77; $[C_5H_4 + H]^+$ m/e = 65; $[C_4H_2 + H]^+$ m/e = 51; $[C_3H_6 + H]^+$ m/e = 43
14.47	$[C_{15}H_{20}O]^+$ m/e = 216	[C14H16O + H]$^+$ m/e = 201; [C13H16 + H]$^+$ m/e = 173; [C12H14 + H]$^+$ m/e = 159; [C11H13 + H]$^+$ m/e = 145; [C10H12]$^+$ m/e = 132; [C9H10 + H]$^+$ m/e = 119; [C8H8 + H]$^+$ m/e = 105; [C7H6 + H]$^+$ m/e = 91; [C6H10 + H]$^+$ m/e = 83; [C6H4 + H]$^+$ m/e = 77; [C5H4 + H]$^+$ m/e = 65; [C4H6 + H]$^+$ m/e = 55
15.07	$[C_{10}H_{10}O_2]^+$ m/e = 162	[C10H10O + H]$^+$ m/e = 147; [C10H12 + H]$^+$ m/e = 133; [C9H10 + H]$^+$ m/e = 119; [C7H6 + H]$^+$ m/e = 91; [C6H4 + H]$^+$ m/e = 77; [C5H4 + H]$^+$ m/e = 65; [C4H6 + H]$^+$ m/e = 55; [C3H6 + H]$^+$ m/e = 43
16.07	$[C_{11}H_{12}O_3]^+$ m/e = 192	$[C_{11}H_{12}O_2 + H]^+$ m/e = 177; $[C_{11}H_{12}O + H]^+$ m/e = 161; $[C_{10}H_{12}O + H]^+$ m/e = 149; $[C_{10}H_9O]^+$ m/e = 145; $[C_9H_{10}O]^+$ m/e = 134; $[C_9H_8 + H]^+$ m/e = 117; $[C_8H_8 + H]^+$ m/e = 105; $[C_7H_4 + H]^+$ m/e = 89; $[C_6H_4 + H]^+$ m/e = 77; $[C_5H_2 + H]^+$ m/e = 63; $[C_4H_2 + H]^+$ m/e = 51; $[C_3H_6 + H]^+$ m/e = 43

used for solving the Eq. (5). the A and E_a were obtained from the plot of $\ln(\frac{g(\alpha)}{T^2})$ vs $\frac{1000}{T}$. The values of a and b were determined from the slope and intercept, respectively, of a straight-line plot between A and E_a. The ln$A$ value was determined by substituting a, b, and average E_a for the specific stage in Eq. 4.

2.4. Pyrolysis GC–MS analysis

The degraded products were collected at 303–583, 583–633, 633–773 and 303–973 K @ 20 K min^{-1} with 5 min hold at every stage, the degradation products were collected in ethanol (15 cm^3) by use of an air-tight assembly (Supplementary Fig. 1) after heating the curcumin samples (~3.63 mg). The collected solutions were injected (1.0 μL) into the GC–MS system in splitless mode. The GC–MS system (Agilent Technologies, USA) consisted of: gas chromatograph GC7890A; mass spectrometer MS5975C with triple-axis detector; HP-5MS column (methylpolysiloxane, 30 m × 250 μm × 0.25 μm). The chromatographic and the mass spectrometric parameters were: helium as carrier gas with 1.0 mL min^{-1} flowrate, 240℃ injector temperature, 4 min solvent delay time, 60℃ for 1 min then 10℃ min^{-1} to 310℃ for 5 min as the column temperatures, 240℃ MS source temperature, 280℃ MSD transfer line temperature, 47 eV relative voltage, mass range 20–700 amu. Data were acquired and processed with the GC/MSD ChemStation® (Agilent Technologies, USA). Compound identification was carried out by comparing mass spectrum of the sample with mass spectral library (NIST 05) of the GC–MS data system.

2.5. Pharmacological properties of degradation products

Pharmacological properties including LD_{50} & LC_{50} values, gastrointestinal absorption, BBB permeation, Cytochrome P450 1A2 inhibitor, CYP2C19 inhibitor, CYP2C9 inhibitor, CYP2D6 inhibitor and CYP3A4 inhibitor were as reported (references given in Table 1) or calculated by use of T.E.S.T (U.S. Environmental Protection Agency, n.d.) and SwissADME Methodologies software (Bioinformatics, n.d.).

3. Results and discussion

The TGA curves at heating rates 5, 10, 15 and 20 K min^{-1} are shown in Fig. 1. It can be seen that curcumin decomposes above 470 K, in two stages at 495–686 K (Stage-I) and 686–894 K (Stage-II). A cursory view of the TGA curves indicates that the degradation occurred in single step, but it may not be true; this can be verified by isoconversional analysis (Starink, 2003). This method requires determination of activation energy (E_a) at different conversions (α). If E_a remains unchanged with change in conversion, the decomposition is said to be a single step and if it changes then the decomposition is regarded as a multistep process.

E_a can be, significantly accurately, determined from the TGA curves obtained at multiple heating rates. In this work we determined activation energy (E_a), pre-exponential factor (A) and degradation mechanism ($g(\alpha)$) using an optimized Kissinger-Akahira-Sunose method (Starink, 2003). E_a was determined from the slope of the Arrhenius plots (Supplementary Fig. 2), the R^2 values of the plots ranged from 0.9997 to 0.9777 (Stage-I) and 0.9869 to 0.986 (Stage-II). The master plots are presented in Fig. 2. The E_a values ~113 kJ mol^{-1} (Stage-I) and ~88 kJ mol^{-1} (Stage-II) suggest that the decomposition at Stage-II occurs quite easily as compared to that at Stage-I. From the TGA data temperature vs conversion (T-α) and activation energy vs conversion (E_a-α) plots were obtained as shown in Fig. 3. The T-α plots indicate that conversion depends on the heating rate. The E_a-α plots indicate a multiple step nature of degradation processes at both the stages as activation energy consistently changes with conversion. This observation is in contrast to earlier findings (Chen et al., 2014). A comparison of the values of frequency factor A (Stage-I: 2.10 × 10^8 s^{-1} and Stage-II: 1.78 × 10^4 s^{-1}) indicate that the reaction rate is faster in Stage-I as compared with that

in Stage-II. The different $g(\alpha)$ models for the two stages, Stage-I: $(1-\alpha)^{-1/2}-1$ and Stage-II: $1-(1-\alpha)^{1/3}$, suggest different mechanisms involved in the degradation processes. After learning, this, we collected degradation products at different temperatures in ethanol and analyzed them by GC–MS.

The decomposition products as identified by GC–MS are listed in Table 1 and typical chromatogram is shown in Fig. 4. The fragmentation patterns of the degradation products are given in Table 2. It was observed that phenol and 2-methoxyphenol are produced at both the stages, i. e., at ambient-1023 K, whereas 1,4-dimethoxy−2-methylbenzene, 1-(2-hydroxy-5-methylphenyl), 4-ethenyl-2-methoxyphenol, 4-ethyl-2-methoxyphenol, 2-methoxy-6-methylphenol, 4-methoxyphenol, 2-methoxy-4-methylphenol, 4-(4-hydroxy-3-methoxyphenyl) but-3-en-2-one, 4-hydroxy-3-methoxybenzaldehyde, 4-(4-hydroxy-3-methoxyphenyl)butan-2-one, 2-methyl-6-(4-methylphenyl)hept-2-en-4-one, 4-(4-hydroxyphenyl)but-3-en-2-one, 2,3-dihydro-1-benzofuran and 3-methylphenol are produced in different temperature ranges (Table. 1). The production of later class confirmed that the decomposition is a multistep process at both the stages. This observation is in line with the results of isoconversional analysis as revealed by typical E_a-α plots (Fig. 3b).

As for as toxicity of the decomposition products is concerned all of these compounds appear to be more toxic (reported/calculated $LD_{50} < 2.56$) than curcumin, whereas 3-methylphenol exhibited higher LD_{50} value (LD_{50}: 2.56). A cursory view of other pharmacological properties of the decomposition products (Table. 1, last column) indicates that all the decomposition products, except 2-methyl-6-(4-methylphenyl)hept-2-en-4-one, can cross the blood–brain barrier (BBB) suggesting that these compounds can adversely affect the brain functions. Twelve of the products including phenol, 1,4-dimethoxy−2-methylbenzene, 1-(2-hydroxy-5-methylphenyl), 4-ethenyl-2-methoxyphenol, 4-ethyl-2-methoxyphenol, 2-methoxy-6-methylphenol, 4-(4-hydroxy-3-methoxyphenyl)but-3-en-2-one, 4-(4-hydroxy-3-methoxyphenyl)butan-2-one, 2-methyl-6-(4-methylphenyl)hept-2-en-4-one, 4-(4-hydroxyphenyl)but-3-en-2-one, 2,3-dihydro-1-benzofuran and 3-methylphenol inhibit cytochrome P450 1A2 in contrast to curcumin. Therefore, these compounds will inhibit the metabolism of xenobiotics. On the other hand, all of the compounds appear to be non-inhibitors of CYP2C9 and CYP3A4 in contrast to curcumin. All of the compounds are non-inhibitors of CYP2C19 and CYP2D6 like curcumin. Thus the experimental evidence provided in this work, suggests that the food materials containing curcumin when heated beyond 470 K will produce toxic substances. So, it is recommended that curcumin should not be heated above this temperature in order to avoid the toxic effects due to the degradation products.

4. Conclusion

This study reveals that curcumin would generate, mostly, toxic degradation products on heating above 470 K. Therefore, the food materials containing curcumin as an ingredient should not be subjected to a cooking process involving heating beyond 470 K.

Funding

The work was not funded by any external agency.

CRediT authorship contribution statement

Rashid Masih: Methodology, Data curation, Validation, Writing – original draft. **Mohammad S. Iqbal:** Validation.

Declaration of Competing Interest

The authors declare that they have no known competing financial interests or personal relationships that could have appeared to influence the work reported in this paper.

Appendix A. Supplementary data

Supplementary data to this article can be found online at https://doi.org/10.1016/j.foodchem.2022.132638.

References

Bioinformatics, S. S. I. of. (n.d.). SwissADME: a web tool to evaluate pharmacokinetics.
Chen, Z., Xia, Y., Liao, S., Huang, Y., Li, Y., He, Y., … Li, B. (2014). Thermal degradation kinetics study of curcumin with nonlinear methods. *Food Chemistry, 155*, 81–86. https://doi.org/10.1016/j.foodchem.2014.01.034
Chengaiah, B., Rao, K. M., Kumar, K. M., Alagusundaram, M., & Chetty, C. M. (2010). Medicinal importance of natural dyes-a review. *International Journal of PharmTech Research, 2*(1), 144–154.
Coat, A. V., & Redfern, J. P. (1964). Kinetic parameters from thermogravimetric data. *Nature, 201*, 68–69.
Dahmke, I. N., Boettcher, S. P., Groh, M., & Mahlknecht, U. (2014). Cooking enhances curcumin anti-cancerogenic activity through pyrolytic formation of "deketene curcumin". *Food Chemistry, 151*, 514–519. https://doi.org/10.1016/j.foodchem.2013.11.102
Esatbeyoglu, T., Ulbrich, K., Rehberg, C., Rohn, S., & Rimbach, G. (2015). Thermal stability, antioxidant, and anti-inflammatory activity of curcumin and its degradation product 4-vinyl guaiacol. *Food and Function, 6*(3), 887–893. https://doi.org/10.1039/c4fo00790e
Iqbal, M. S., Khan, M. U. A., Akbar, J., Shad, M. A., Masih, R., & Chaudhary, M. T. (2016). Isoconversional thermal and pyrolytic GC–MS analysis of street samples of hashish. *Journal of Analytical and Applied Pyrolysis., 122*, 175–182. https://doi.org/10.1016/j.jaap.2016.09.026
Janković, B. (2008). Kinetic analysis of the nonisothermal decomposition of potassium metabisulfite using the model-fitting and isoconversional (model-free) methods. *Chemical Engineering Journal, 139*(1), 128–135. https://doi.org/10.1016/j.cej.2007.07.085
Nelson, K. M., Dahlin, J. L., Bisson, J., Graham, J., Pauli, G. F., & Walters, M. A. (2017). The essential medicinal chemistry of curcumin. *Medicinal Chemistry, 60*, 1620–1637. https://doi.org/10.1021/acs.jmedchem.6b00975
Shang, Z. P., Xu, L. L., Lu, Y. Y., Guan, M., Li, D. Y., Le, Z. Y., … Ye, M. (2019). Advances in chemical constituents and quality control of turmeric. *World Journal of Traditional Chinese Medicine, 5*(2), 116–121. https://doi.org/10.4103/wjtcm.wjtcm_12_19
Starink, M. J. (2003). The determination of activation energy from linear heating rate experiments: A comparison of the accuracy of isoconversion methods. *Thermochimica Acta, 404*(1–2), 163–176. https://doi.org/10.1016/S0040-6031(03)00144-8
Turmanova, S. C., Genieva, S. D., Dimitrova, A. S., & Vlaev, L. T. (2008). Non-isothermal degradation kinetics of filled with rise husk ash polypropene composites. *Express Polymer Letters, 2*(2), 133–146. https://doi.org/10.3144/expresspolymlett.2008.18
U.S. Environmental Protection Agency. (n.d.). Toxicity Estimation Software Tool.
Volate, S. R., Davenport, D. M., Muga, S. J., & Wargovich, M. J. (2005). Modulation of aberrant crypt foci and apoptosis by dietary herbal supplements (quercetin, curcumin, silymarin, ginseng and rutin). *Carcinogenesis, 26*(8), 1450–1456. https://doi.org/10.1093/carcin/bgi089
Vyazovkin, S., Burnham, A. K., Criado, J. M., Pérez-Maqueda, L. A., Popescu, C., & Sbirrazzuoli, N. (2011). ICTAC Kinetics Committee recommendations for performing kinetic computations on thermal analysis data. *Thermochimica Acta, 520*(1–2), 1–19. https://doi.org/10.1016/j.tca.2011.03.034